http://dx.doi.org/10.5012/bkcs.2013.34.3.773

Synthesis and Characterization of 1-D BiSI and 2-D BiOI Nanostructures

Juheon Lee, Bong-Ki Min,† Insu Cho, and Youngku Sohn*

*Department of Chemistry, Yeungnam University, Gyeongsan 712-749, Korea. *E-mail: youngkusohn@ynu.ac.kr*
†Center for Research Facilities, Yeungnam University, Gyeongsan 712-749, Korea
Received October 9, 2012, Accepted December 8, 2012

We have prepared 1-D BiSI and 2-D BiOI nanostructures, and characterized them by scanning electron microscopy, transmission electron microscopy (TEM), X-ray diffraction crystallography, thermogravimetric analysis/differential scanning calorimetry, and UV-visible absorption. Here, we first report clear HR-TEM image of BiSI. In addition, we first found that the growth direction of BiSI is [12-1] plane, with the neighboring distance of 0.30 nm. The crystal structures of BiSI and BiOI are found to be orthorhombic (Pnam) and tetragonal (P4/nmm), respectively. The absorption band gaps of BiSI and BiOI are measured to be 1.55 and 1.92 eV, respectively. Our study could further highlight the applications of V-VI-VII compounds.

Key Words : BiSI, BiOI, Growth direction, TEM, Band-gap

Introduction

Bismuth sulfur iodide (BiSI) is one among V-VI-VII (or 15-16-17) compounds.[1-5] Although the compound shows many interesting properties such as ferroelectric, photoelectric, and piezoelectric there have been few fundamental studies.[4-10] Single crystal BiSI has generally been prepared by a vapor-phase method.[10,11] Recently, mild condition methods (*e.g.*, hydrothermal and solvothermal methods) have been employed to synthesize BiSI, where rod-like orthorhombic structures are commonly formed.[6-9] Fa *et al.*, employed a solvothermal method with Bi nitrate, thiourea and iodine dissolved in ethanol at 160 ºC for 30 h.[8] Wang *et al.* prepared BiSI films by an ultrasonic spray pyrolysis method at 320 ºC using $BiCl_3$, thiourea and iodide.[12] They could control the growth direction of BiSI by controlling the interval time between spray pulses. Kumar *et al*. employed a gel technique to obtain 5 mm long BiSI single crystals.[13] On the other hand, BiOI (the same V-VI-VII class compound) has widely been studied in recent years,[14-28] especially because of a high catalytic activity in the visible region. BiOI has been reported to show a high photocatalytic activity for photodegradation of an organic dye under visible light irradiation.[26-28] For a dye removal, BiOI has been proved to be more active than that of bulk TiO_2 under visible light.[27] In this paper, we have focused more on few studied BiSI, and further fundamentally characterize BiSI prepared by a hydrothermal method. Here, we first report very clear HR-TEM image of 1-D BiSI and the growth direction of the rod, which is not reported in previous literatures.[6-9,12,13]

Experimental

For the synthesis of mixed BiSI and BiOI, stoichiometric amounts of $BiCl_3$ (Sigma-Aldrich, 99.9%), I_2, and thiourea were transferred into a 100 mL Teflon-lined stainless autoclave with 70 mL Millipore water (18.2 MΩ-cm resistivity).[6] The autoclave was placed in an oven (200 ºC) for 24 h. The final precipitates were washed with water and ethanol several times, and dried in an oven (80 ºC) for a day. Because BiOI is soluble in a dilute hydrochloric acid solution, we could obtain pure BiSI by washing the as-prepared product with a dilute HCl solution. To examine the crystal structures of the samples we used PANalytical X'Pert Pro MPD diffractometer with Cu Kα radiation to take X-ray diffraction (XRD) patterns. The surface morphology was taken by scanning electron microscopy (SEM, Hitachi S-4800). TEM and high resolution TEM (HR-TEM) images of 1-D BiSI were taken using a FEI Tecnai G2 F20 microscope at 200 kV. Diffuse reflectance spectra were recorded using a UV-Vis spectrophotometer (Cary 5000). Thermogravimetric analysis/Differential Scanning Calorimetry (TGA/DSC) were carried using a TA Instruments thermal analyzer at a temperature heating rate of 10 °C/min under air condition.

Results and Discussion

The SEM images of the as-prepared product (BiSI and BiOI) are displayed in Figure 1. Upon completion of the hydrothermal reaction at 200 ºC, we found two different shapes (Figure 1(a)); plates (or nanowalls) and rods, where the plates cover the rods. The two products could be separated into pure rod-shape BiSI (Figure 1(b)) and wall-type BiOI (Figure 1(c)). The 1-dimensional (1-D) BiSI structures are 10-120 μm long and 0.4-2.6 μm thick with an aspect ratio of 30-40. The wall structures for BiOI are found to be 100 nm thick and ~2 μm wide.

Figure 2 shows the XRD patterns and their corresponding crystal planes for the two different structures. The bottom XRD peaks are in very good matching with the patterns of orthorhombic (Pnam) structure (JCPDS 043-0652, a = 8.51 Å, b = 10.26 Å, c = 4.17 Å) for BiSI. The major peaks are found at 2θ = 20.20º, 22.6º, 29.50º, and 32.73º, corresponding to [120], [210], [121], and [310] planes. Fang *et al.*

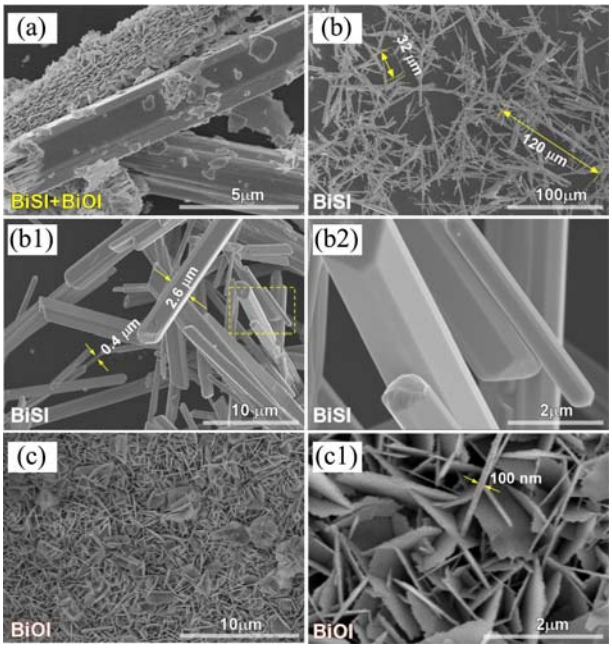

Figure 1. SEM images of as-prepared mixed products (a), and purified BiSI (b, b1 and b2) and BiOI (c and c1).

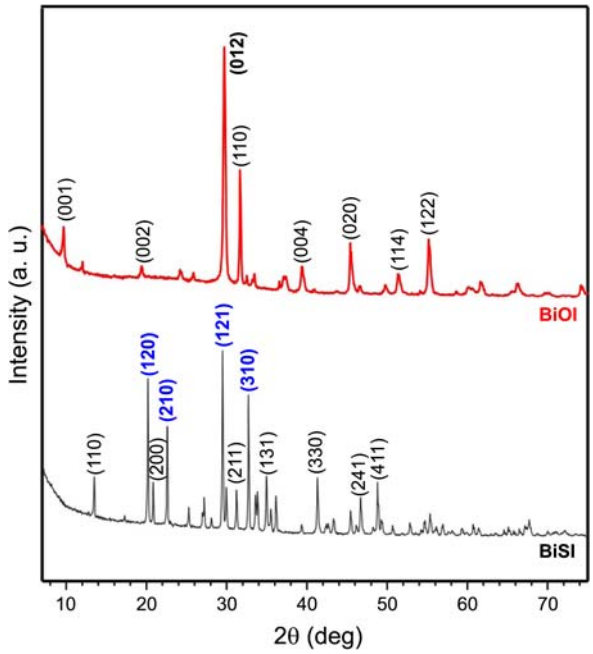

Figure 2. Powder X-ray diffraction patterns of 1-D BiSI and 2-D BiOI. The major crystal planes are assigned on the peaks, and other minors are omitted for clarity.

prepared BiSI with 50-80 nm wide and 1-3 μm long (aspect ratios of 20-40), and obtained the XRD patterns of orthorhombic (Pnam) structure (JCPDS 043-0652), in good agreement with our result. The other XRD patterns (top) are quite different from those of BiSI, and are those of tetragonal (P4/nmm) structure (JCPDS 00-073-2062, a = b = 3.98 Å, c = 9.13 Å) of BiOI. The strongest peak at 2θ = 29.70º corresponds to [012] plane. For lamella BiOI prepared by Fang *et al.*, the dominant peak was found to be [004] plane, and other dominant peaks were assigned to [002] and [102] planes.[7] Fa *et al.*, used ethanol as a solvent in stead of using water for the synthesis of BiSI.[8] Other recipes are the same as ours. They found that BiOI and BiSI are both competitive reaction products depending on the mole ratio of thiourea/Bi nitrate. When the ratios were 1, and > 2, they obtained dark red-orange BiOI nanomellas, and BiSI nanowires, respectively.

A typical TEM image is shown in Figure 3. The1-D BiSI rod is smooth and straight. The HR-TEM image shows a clear lattice image indicating a single-crystalline structure of the rod. The edge of the rod shows an amorphous layer of about 3 nm thick in our observation. In the HR-TEM image, the distance of about 0.30 nm between the arrow-heads corresponds to the distance of [12-1] planes, the growth direction of the rod indicated by a green arrow. The distance of 0.32 nm corresponds to the neighboring distance of [2-20] planes. The indexed Fourier transform of the image is oriented close to the [113] direction. The growth direction of a 1-D BiSI rod is found to be [12-1] direction.

Figure 4 displays the UV-visible absorption spectra of the two samples, and their photo images showing colors; reddish-brown and dark-gray for BiOI and BiSI, respectively. The absorbance (y-axis) is converted from the diffuse reflectance

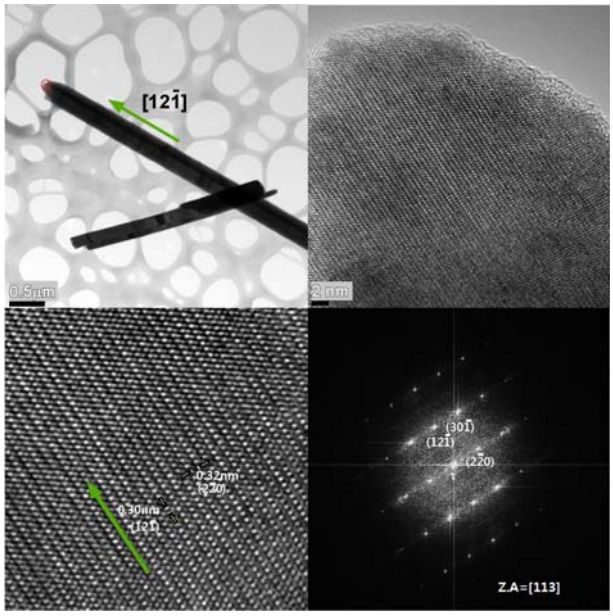

Figure 3. TEM, HRTEM images, and the FFT patterns of 1-D BiSI structure.

by the Kubelka-Munk method. The band gap is estimated using $(\alpha h\nu)^n = A(h\nu - E_g)$, where A is an empirical constant, α is absorption coefficient, and n = 1/2 for an indirect interband transition for BiOI and BiSI.[10,27] We re-plot $[KM]^{1/2}$ *versus* hν (not shown) from the spectra of Figure 4, and determine the absorption edge by the intersection of the two straight lines (from $[KM]^{1/2}$ and hν). The cross absorption edges for BiSI and BiOI are determined to be 1.55 and 1.92 eV, respectively. Fang *et al.* reported optical band gaps of 1.61 and 1.97 eV for BiSI (50-80 nm wide and 1-3 μm

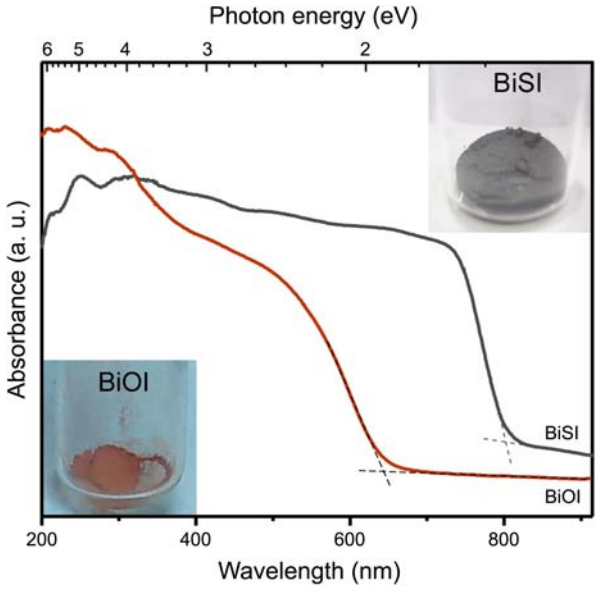

Figure 4. UV-visible diffuse reflectance absorption spectra of BiSI and BiOI. Digital camera images show the colors (dark-gray and reddish-brown) of the two samples.

long) and BiOI prepared by a solvothermal method, respectively.[7] For rod-like BiSI prepared by a hydrothermal method, Su *et al.* observed an absorption edge at around 820 nm (1.51 eV; in good agreement with ours), but they reported a band gap of 1.8 eV.[6] It is known that the difference in band gap of a material is due to difference in crystal morphology, size, crystallinity, and uniformity. In addition, the deviation could be originated from the method for the determination of a band gap edge (or intersection), and the instrumental error. For this reason, in many cases it is difficult to choose the main reason of showing a different band gap. Table 1 summarizes some literature values for the band gaps of BiOI and BiSI.

Figure 5 displays the TG/DSC analysis curves of 1-D BiSI, recorded with a heating rate of 10 °C/min in air. Upon heating in air condition, no critical change in weight occurs until the temperature reaches to 350 ºC. Above this temperature a dramatic change in weight occurs up to 550 ºC. A sharp exothermic peak is found at 425 ºC. The total weight loss is measured to be 40%. For BiOI reported by Yu *et al.* BiOI decomposes upon heating above 350 ºC in air condition.[28] From 350 ºC to 520 ºC, they proposed a plausible

Table 1. Some literature values for the band gaps of BiOI and BiSI

Sample	Band gap	Morphology	Ref.
BiOI	1.87	nanoplates	21
	1.84	flower-like porous microspheres (2-3 μm diameter)	28
	1.97	nanolamellas	7
	1.72	Plates (0.1-2 μm diameter)	27
	1.77	Solvothermal method(ethylene glycol) hierarchical microspheres consisting of nanoplates (2-5 μm diameter)	20
	1.92	**2-D-nanowalls**	This work
BiSI	1.61	Rod like: 50-80 nm wide, 1-3 μm long	7
	1.55	**Rod-like 1-D-structure**	This work

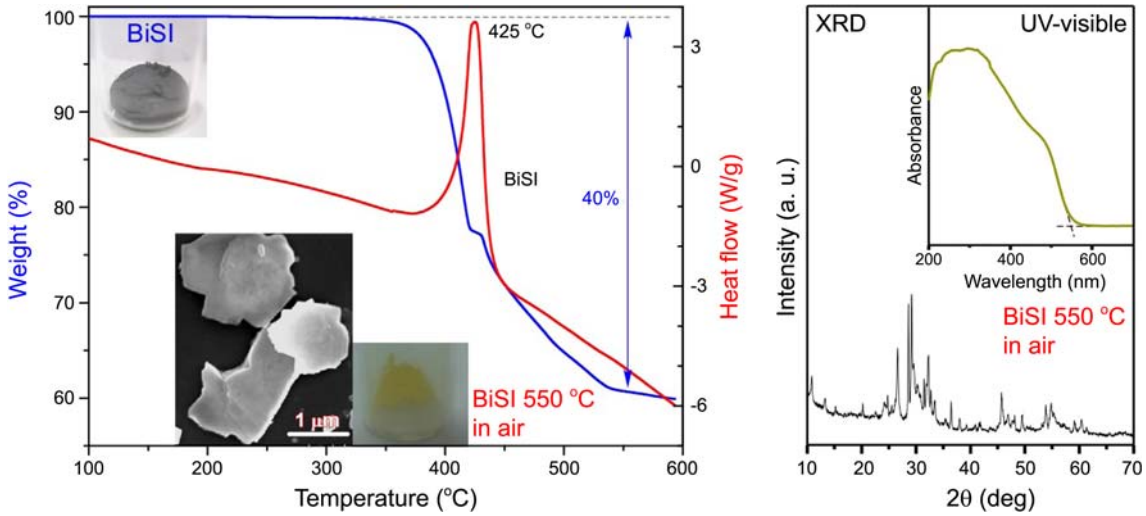

Figure 5. TG/DSC analysis curves of 1-D BiSI (left). The change in color is shown by the photo images. Inset shows a SEM image after annealing. XRD (right) and UV-visible absorption spectra (inset, right) of BiSI upon 550 ºC annealing in an air condition.

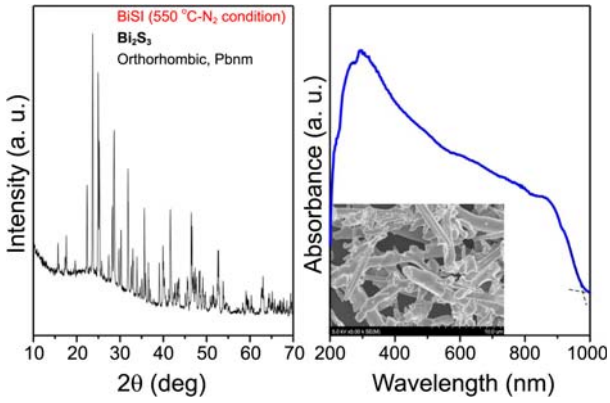

Figure 6. XRD (left) and UV-Visible absorption spectrum (right) of BiSI upon 550 ºC annealing in nitrogen condition. Inset (right) shows a SEM image after annealing.

decomposition reaction; $5BiOI + O_2 \rightarrow Bi_5O_7I + 2I_2$. Upon further heating above 700 ºC, it was reported to transform to α-Bi_2O_3 based on TG and XRD data.[29] In nitrogen condition, it was reported that BiSI thermally decomposes to iodine-deficient $Bi_{19}S_{27}I_3$ upon annealing above 425 ºC. The compound further decomposes to Bi_2S_3 upon further heating above 650 ºC.[30] During the decomposition process, BiI_3 is formed as vapor. To confirm the formation of Bi_2S_3 in a nitrogen condition, we took XRD patterns, UV-visible absorption spectrum, and SEM image (Figure 6) for the 1-D BiSI annealed at 550 ºC in a nitrogen condition. We found the XRD patterns are those of orthorhombic (Pbnm) structure (JCPDS 017-0320) of Bi_2S_3. The band gap was measured to be 1.27 eV, in good agreement with the literature value.[31]

Conclusion

In summary, 1-D BiSI (rod) and 2-D BiOI (wall) nanostructures were successfully prepared by a hydrothermal method, and fully characterized by SEM, HR-TEM, XRD, UV-visible absorption, and TG/DSC analysis. The growth direction of 1-D BiSI is found to be [12-1], and the neighboring distance of the planes is measured to be 0.30 nm. The UV-visible absorption spectra reveal that the band gaps of 1-D BiSI and 2-D BiOI are measured to 1.55 and 1.92 eV, respectively. The decomposition of BiSI starts to occur at around 350 ºC on the basis of TG data. In a nitrogen condition, BiSI decomposes to Bi_2S_3 with a measured band gap of 1.27 eV, upon annealing at 550 ºC. Our detailed studies could further highlight the fundamental characteristics and applications of V-VI-VII compounds.

Acknowledgments. This research was supported by the Yeungnam University research grants in 2010.

References

1. Horak, E.; Cermak, J.; Czech, K. *J. Phys. B* **1965**, *15*, 536.
2. Audzijonis, S.; Mykolaitiene, A.; Grigas, N.; J. *Ferroelectrics* **1996**, *77*, 181.
3. Whatmore, R. W. *Rep. Prog. Phys.* **1986**, *49*, 1335.
4. Audzijonis, A.; Gaigalas, G.; Zigas, L.; Pauliukasa, A.; Zaltauskas, R.; Cerskus, A.; Narusis J.; Kvedaravicius, A. *Physica B* **2007**, *391*, 22.
5. Audzijonis, A.; Žaltauskas, R.; Sereika, R.; Žigas, L.; Rëza, A. *J. Phys. Chem. Solids* **2010**, *71*, 884.
6. Su, X.; Zhang, G.; Liu, T.; Liu, Y.; Qin, J.; Chen, C. *Russ. J. Inorg. Chem.* **2006**, *51*, 1864.
7. Fang, F.; Linga, C.; Li-Ming, W. *Chinese J. Struct. Chem.* **2009**, *28*, 1399.
8. Fa, W. J.; Li, P. J.; Zhang, Y. G.; Guo, L. L.; Guo, J. F.; Yang, F. L. *Advanced Materials Research* **2011**, *1919*, 236.
9. Zhu, L. Y.; Xie, Y.; Zheng, X. W.; Yin, X.; Tian, X. B. *Inorg. Chem.* **2001**, *41*, 4560.
10. Grigas, J.; Talik, E.; Adamiec, M.; Lazauskas, V.; Nelkinas, V. *J. Electron Spectrosc. Rel. Phenom.* **2006**, *153*, 22.
11. Arivuoli, D.; Gnanam, F. D.; Ramsamy, P. *J. Mater. Sci.* **1986**, *21*, 2835.
12. Wang, W.; Wang, S. Y.; Liu, M. *Materials Research Bulletin* **2005**, *40*, 1781.
13. Kumar, R. R.; Raman, G.; Gnanam, F. D. *J. Mater. Sci.* **1989**, *24*, 4531.
14. Wang, W. D.; Huang, F. Q.; Lin, X. P.; Yang, J. H. *Catal. Commun.* **2008**, *9*, 8.
15. An, H. Z.; Du, Y.; Wang, T. M.; Wang, C.; Hao, W. C.; Zhang, J. Y. *Rare Metals* **2008**, *27*, 243.
16. Zhao, K.; Zhang, X.; Zhang, L. Z. *Electrochem. Commun.* **2009**, *11*, 612.
17. Henle, J.; Simon, P.; Frenzel, A.; Scholz, S.; Kaskel, S. *Chem. Mater.* **2007**, *19*, 366.
18. Zhang, X.; Zhang, L. Z.; Xie, T. F.; Wang, D. J. *J. Phys. Chem. C* **2009**, *113*, 7371.
19. Chang, X. F.; Huang, J.; Tan, Q. Y.; Wang, M.; Ji, G. B.; Deng, S. B.; Yu, G. *Catal. Commun.* **2009**, *10*, 1957.
20. Zhang, X.; Ai, Z. H.; Jia, F. L.; Zhang, L. Z. *J. Phys. Chem. C* **2008**, *112*, 747.
21. Xiao, X.; Zhang, W. D. *J. Mater. Chem.* **2010**, *20*, 5866.
22. Lei, Y. Q.; Wang, G. H.; Song, S. Y.; Fan, W. Q.; Pang, M.; Tang, J. K.; Zhang, H. J. *Dalton Trans.* **2010**, *39*, 3273.
23. Xia, J. X.; Yin, S.; Li, H. M.; Xu, H.; Yan, Y. S.; Qi, Z. *Langmuir* **2011**, *27*, 1200.
24. Zhang, K. L.; Liu, C. M.; Huang, F. Q.; Zheng, C.; Wang, W. D. *Appl. Catal., B* **2006**, *68*, 125.
25. Song, L.; Zhang, S.; Wei, Q. *Ind. Eng. Chem. Res.* **2012**, *51*, 1193.
26. Chang, X.; Huang, J.; Cheng, C.; Sui, Q.; Sha, W.; Ji, G.; Deng, S.; Yu, G. *Catal. Commun.* **2010**, *11*, 460.
27. Cao, J.; Xu, B.; Luo, B.; Lin, H.; Chen, S. *Catal. Commun.* **2011**, *13*, 63.
28. Xia, J.; Yina, S.; Li, H.; Xub, H.; Xua, L.; Zhang, Q. *Colloid Surface A* **2011**, *387*, 23.
29. Yu, C.; Fan, C.; Yu, J. C.; Zhou, W.; Yang, K. *Mater. Res. Bull.* **2011**, *46*, 140.
30. Kramer, V. J. *Therm. Anal.* **1979**, *16*, 295.
31. Zhang, Z.; Wang, W.; Wang, L.; Sun, S. *ACS Appl. Mater. Interfaces* **2012**, *4*, 593597.